Neutron Powder Diffraction Study on the Crystal and Magnetic Structures of $BiCoO_3$

Alexei A. Belik,*,† Satoshi Iikubo,‡ Katsuaki Kodama,‡ Naoki Igawa,‡ Shin-ichi Shamoto,‡ Seiji Niitaka,§ Masaki Azuma,§,|| Yuichi Shimakawa,§ Mikio Takano,§ Fujio Izumi,⊥ and Eiji Takayama-Muromachi⊥

International Center for Young Scientists (ICYS) and Advanced Materials Laboratory (AML), National Institute for Materials Science (NIMS), 1-1 Namiki, Tsukuba, Ibaraki 305-0044, Japan, Neutron Science Research Center, Japan Atomic Energy Research Institute, Tokai, Ibaraki 319-1195, Japan, Institute for Chemical Research, Kyoto University, Uji, Kyoto-fu 611-0011, Japan, and PRESTO, Japan Science and Technology Corporation (JST), Kawaguchi, Saitama 332-0012, Japan

Received October 24, 2005. Revised Manuscript Received December 7, 2005

The crystal and magnetic structures of polycrystalline $BiCoO_3$ have been determined by the Rietveld method from neutron diffraction data measured at temperatures from 5 to 520 K. $BiCoO_3$ (space group *P*4*mm*; $Z = 1$; $a = 3.72937(7)$ Å and $c = 4.72382(15)$ Å at room temperature; tetragonality $c/a = 1.267$) is isotypic with $BaTiO_3$ and $PbTiO_3$ in the whole temperature range. $BiCoO_3$ is an insulator with a Néel temperature of 470 K. A possible model for antiferromagnetic order is proposed with a propagation vector of $\mathbf{k} = (1/2, 1/2, 0)$. In this model, magnetic moments of Co^{3+} ions are parallel to the *c* direction and align antiferromagnetically in the *ab* plane. The antiferromagnetic *ab* layers stack ferromagnetically along the *c* axis, forming a C-type antiferromagnetic structure. Refined magnetic moments at 5 and 300 K are $3.24(2)\mu_B$ and $2.93(2)\mu_B$, respectively. The structure refinements revealed no deviation from stoichiometry in $BiCoO_3$. $BiCoO_3$ decomposed in air above 720 K to give Co_3O_4 and sillenite-like $Bi_{25}CoO_{39}$.

Introduction

Multiferroic materials have received renewed interest in recent years.[1] In multiferroic systems, two or all three of (anti)ferroelectricity, (anti)ferromagnetism, and ferroelasticity are observed in the same phase.[2] Such systems are rare in nature[2] but potentially studied with interest in wide technological applications.[3−5] Many efforts have been devoted to preparing new materials with multiferroic properties[5] and to finding multiferroic properties in known compounds.[3,4,6]

One direction in searching for new multiferroic materials is to combine ferroelectric materials, e.g., $PbTiO_3$ and $BaTiO_3$, with magnetic materials, e.g., $BiFeO_3$ and $CoFe_2O_4$.[7−9] Solid solutions including $PbTiO_3$ as the end member, for example, $PbTiO_3-BiMO_3$,[9−12] were extensively studied in attempts to synthesize new multiferroics, improve ferroelectric properties of $PbTiO_3$ by increasing the tetragonality, *c*/*a* (*a* and *c* are lattice parameters), reduce the content of lead, and find new morphotropic phase boundary piezoelectrics. Another direction is to combine Pb^{2+} and Bi^{3+} ions with lone electron pairs and magnetic ions such as d electron systems.[5]

In the course of searching for new multiferroics, two simple oxides $Pb^{4+}V^{4+}O_3$ and $Bi^{3+}Co^{3+}O_3$,[13,14] which possess the $PbTiO_3$-type structure and magnetic ions, have been found. The tetragonality of $PbVO_3$ ($c/a = 1.23$) or $BiCoO_3$ ($c/a = 1.27$) is much larger than that of $PbTiO_3$ ($c/a = 1.06$),

* To whom correspondence should be addressed: International Center for Young Scientists (ICYS), National Institute for Materials Science (NIMS), 1-1 Namiki, Tsukuba, Ibaraki 305-0044, Japan. Tel: +81 (029) 851-3354 (ext. 8587). Fax: +81 (029) 860-4706. E-mail: Alexei.BELIK@nims.go.jp.
† ICYS, NIMS.
‡ Japan Atomic Energy Research Institute.
§ Kyoto University.
|| JST.
⊥ AML, NIMS.

(1) For recent reviews see (a) Fiebig, M. *J. Phys. D: Appl. Phys.* **2005**, *38*, R123. (b) Prellier, W.; Singh, M. P.; Murugavel, P. *J. Phys.: Condens. Matter* **2005**, *17*, R803. (c) Hill, N. A. *Annu. Rev. Mater. Res.* **2002**, *32*, 1.
(2) Hill, N. A. *J. Phys. Chem. B* **2000**, *104*, 6694.
(3) Kimura, T.; Goto, T.; Shintani, H.; Ishizaka, K.; Arima, T.; Tokura, Y. *Nature* **2003**, *426*, 55.
(4) Hur, N.; Park, S.; Sharma, P. A.; Ahn, J. S.; Guha, S.; Cheong, S.-W. *Nature* **2004**, *429*, 392.
(5) Azuma, M.; Takata, K.; Saito, T.; Ishiwata, S.; Shimakawa, Y.; Takano, M. *J. Am. Chem. Soc.* **2005**, *127*, 8889.
(6) Lawes, G.; Harris, A. B.; Kimura, T.; Rogado, N.; Cava, R. J.; Aharony, A.; Entin-Wohlman, O.; Yildirim, T.; Kenzelmann, M.; Broholm, C.; Ramirez, A. P. *Phys. Rev. Lett.* **2005**, *95*, 087205.
(7) Zheng, H.; Wang, J.; Lofland, S. E.; Ma, Z.; Mohaddes-Ardabili, L.; Zhao, T.; Salamanca-Riba, L.; Shinde, S. R.; Ogale, S. B.; Bai, F.; Viehland, D.; Jia, Y.; Schlom, D. G.; Wuttig, M.; Roytburd, A.; Ramesh, R. *Science* **2004**, *303*, 661.
(8) (a) Woodward, D. I.; Reaney, I. M.; Eitel, R. E.; Randall, C. A. *J. Appl. Phys.* **2003**, *94*, 3313. (b) Comyn, T. P.; McBride, S. P.; Bell, A. J. *Mater. Lett.* **2004**, *58*, 3844.
(9) (a) Wang, N.; Cheng, J.; Pyatakov, A.; Zvezdin, A. K.; Li, J. F.; Cross, L. E.; Viehland D. *Phys. Rev. B* **2005**, *72*, 104434. (b) Kanai, T.; Ohkoshi, S.; Nakajima, A.; Watanabe, T.; Hashimoto, K. *Adv. Mater.* **2001**, *13*, 487.
(10) Iniguez, J.; Vanderbilt, D.; Bellaiche, L. *Phys. Rev. B* **2003**, *67*, 224107.
(11) (a) Zhang, S. J.; Randall, C. A.; Shrout, T. R. *Appl. Phys. Lett.* **2003**, *83*, 3150. (b) Sterianou, I.; Reaney, I. M.; Sinclair, D. C.; Woodward, D. I.; Hall, D. A.; Bell, A. J.; Comyn, T. P. *Appl. Phys. Lett.* **2005**, *87*, 242901.
(12) (a) Inaguma, Y.; Miyaguchi, A.; Yoshida, M.; Katsumata, T.; Shimojo, Y.; Wang, R. P.; Sekiya, T. *J. Appl. Phys.* **2004**, *95*, 231. (b) Cheng, J. R.; Meng, Z. Y.; Cross, L. E. *J. Appl. Phys.* **2005**, *98*, 084102.
(13) Belik, A. A.; Azuma, M.; Saito, T.; Shimakawa, Y.; Takano, M. *Chem. Mater.* **2005**, *17*, 269.

10.1021/cm052334z CCC: $33.50
Published on Web 01/11/2006

which suggests very large spontaneous polarization. First-principle Berry-phase calculations predicted electric polarizations of 152 μC/cm^2 in $PbVO_3$ and 179 μC/cm^2 in $BiCoO_3$.[15] The electrical resistivity of $BiCoO_3$ exhibited activation-type temperature dependence but was as low as 10^{-2} Ω-cm at room temperature (RT).[14] The Néel temperature (T_N) of $BiCoO_3$ was reported to be 470 K from magnetic susceptibility measurements.[14] The magnetism of $PbVO_3$ still needs to be clarified because no magnetic reflections appeared in neutron powder diffraction patterns down to 1.5 K[16] and no anomaly characteristic of long-range order was observed in specific heat capacities at temperatures from 400 to 0.4 K.[13]

In this work, we determined the crystal and magnetic structures of $BiCoO_3$ by the Rietveld method from neutron powder diffraction data measured at 5, 300, 450, and 520 K. Neutron diffraction unambiguously confirmed the onset of long-range antiferromagnetic order below T_N and allowed us to acquire detailed structure information about $BiCoO_3$ in a wide temperature range.

Experimental Section

Synthesis. A mixture of Bi_2O_3 (99.99%), Co_3O_4 (99.9%), and $KClO_3$ (99.5%) with an amount-of-substance ratio of 9:6:1 was placed in Au capsules and treated at 6 GPa in a belt-type high-pressure apparatus at 1243 K for 100 min. $KClO_3$ was added as an oxygen generator and put at the bottom and top of each capsule. After heat treatment, the samples were quenched to RT, and the pressure was slowly released. Surfaces of the resultant black and hard pellets were removed using sandpaper. X-ray powder diffraction (XRD) showed the inclusion of Co_3O_4 and a small amount of $Bi_2O_2CO_3$, and very weak reflections of unidentified impurities in addition to the main phase of $BiCoO_3$.

Scanning Electron Microscopy (SEM) and Energy Dispersive X-ray (EDX) Analysis. SEM-EDX analysis was performed using an Hitachi S-4800 scanning electron microscope, equipped with an EDX spectrometer (Horiba, EMAX).

Thermal Analysis. The thermal stability of $BiCoO_3$ in air was examined on a SII Exstar 6000 (TG-DTA 6200) system between RT and 970 K at a heating−cooling rate of 10 K/min using Pt holders. Differential scanning calorimetry (DSC) curves of $BiCoO_3$ in closed aluminum capsules were recorded between 140 and 523 K at a heating−cooling rate of 10 K/min on a SII Exstar 6000 (DSC 6220) instrument.

Magnetic and Transport Properties. Magnetic susceptibilities, $\chi = \mathbf{M}/\mathbf{H}$, of $BiCoO_3$ were measured on a SQUID magnetometer (Quantum Design, MPMS) between 330 and 520 K (and 600 K) in an applied field of 50 kOe. Electrical resistivities were measured between 385 and 400 K (with a resistivity of about 10^5 Ω-cm at 400 K) by the conventional four-probe method using a PPMS instrument (Quantum Design) with an *ac*-gage current of 0.01 mA at 30 Hz. At lower temperatures down to 10 K, the resistivity was too large to be measured with our system. Because of the measurements near the limit of sensitivity in our system, no definite activation energy could be deduced from the data (see Supporting Information).

Neutron Powder Diffraction Experiments and Structure Refinements. Neutron powder diffraction data of $BiCoO_3$ were collected at 5, 300, 450, and 520 K (starting from the lowest temperature) with the high-resolution powder diffractometer (HRPD) installed at the JRR-3M reactor in JAERI, Tokai. The incident neutron wavelength was 1.8233(10) Å. About 6.2 g of the sample was contained in a V holder (diameter: 6.0 mm) filled with He. A cryostat containing the holder was slowly oscillated during the measurement. The data were taken with a step of ca. 0.05° in a 2θ range between 2.5 and 162° with 64 ^{3}He detectors. The measurement time was 20 h at 520 K and 10 h at the other temperatures.

The neutron powder diffraction data were analyzed by the Rietveld method with RIETAN-2000.[17] The background was represented by an eighth-order Legendre polynomial. The pseudo-Voigt function of Thompson et al.[18] was used as a profile function. Profile asymmetry was represented according to the procedure of Finger et al.[19] Isotropic atomic displacement parameters, U, with the isotropic Debye−Waller factor represented as $\exp(-8\pi^2 U \sin^2\theta/\lambda^2)$ were assigned to all the sites. Bound coherent scattering lengths, b_c, used for the structure refinements were 8.532 fm (Bi), 2.49 fm (Co), and 5.803 fm (O).[20] Coefficients for analytical approximations to the magnetic form factor of Co^{3+} were taken from ref 21.

Results

Magnetic Properties and Thermal Stability of $BiCoO_3$. Figure 1a shows magnetic susceptibilities of $BiCoO_3$ between 330 and 600 K. The maximum in the $\chi(T)$ curves was observed near $T_N = 470$ K, which confirms the antiferromagnetic phase transition. When the $\chi(T)$ curves on heating and cooling were measured between 330 and 520 K; both of them were almost the same. However, if the sample was heated to 600 K, the heating and cooling curves did not coincide with each other. This fact indicates that the oxygen content of the sample slightly changed at 600 K. Such a deviation from stoichiometry prevents us from estimating the effective magnetic moment unambiguously above T_N. The magnetic phase transition was also detected at 470 K as a bend of the DSC and DTA curves (Figure 1).

The TG/DTA data showed a small step of weight loss above 600 K with a small endothermal effect (Figure 1b). A strong exothermal effect started from 720 K, accompanied by weight gain and further weight loss between 740 and 900 K. XRD showed that the resultant decomposed sample consisted of only two phases, Co_3O_4 and sillenite-like "$Bi_{25}CoO_{39}$". Because sillenite-like phases have variable compositions,[22] the chemical formula of "$Bi_{25}CoO_{39}$" is not exact.

Refinements of Crystal and Magnetic Structures for $BiCoO_3$. All the reflections of $BiCoO_3$ at 520 K could be

(14) (a) Niitaka, S.; Azuma, M.; Takano, M.; Nishibori, E.; Takata, M.; Sakata, M. *Meeting Abstracts of the Physical Society of Japan*, 59th Annual Meeting, March 27−30, 2004, Kyushu University; The Physical Society of Japan: Tokyo, Japan, 2004; Vol. 59, Issue 1, Part 3, p 511 (ISSN 1342-8349). (b) Azuma, M.; Niitaka, S.; Belik, A. A.; Ishiwata, S.; Kanda, H.; Yamada, I.; Takano M. *4th International Conference on Inorganic Materials*, Antwerp, Belgium, September 19−21, 2004, Book of Abstracts; Elsevier: Amsterdam, 2004; p 204.
(15) Uratani, Y.; Shishidou, T.; Ishii, F.; Oguchi, T. *Jpn. J. Appl. Phys. Part 1* **2005**, *44*, 7130.
(16) Shpanchenko, R. V.; Chernaya, V. V.; Tsirlin, A. A.; Chizhov, P. S.; Sklovsky, D. E.; Antipov, E. V.; Khlybov, E. P.; Pomjakushin, V.; Balagurov, A. M.; Medvedeva, J. E.; Kaul, E. E.; Geibel, C. *Chem. Mater.* **2004**, *16*, 3267.
(17) Izumi, F.; Ikeda, T. *Mater. Sci. Forum* **2000**, *321−324*, 198.
(18) Thompson, P.; Cox, D. E.; Hastings, J. B. *J. Appl. Crystallogr.* **1987**, *20*, 79.
(19) Finger, L. W.; Cox D. E.; Jephcoat, A. P. *J. Appl. Crystallogr.* **1994**, *27*, 892.
(20) Sears, V. F. *International Tables for Crystallography*, 3rd ed.; Kluwer: Dordrecht, 2004; Vol. C, pp 445−452.
(21) Brown, P. J. *International Tables for Crystallography*, 3rd ed.; Kluwer: Dordrecht, 2004; Vol. C, p 454.

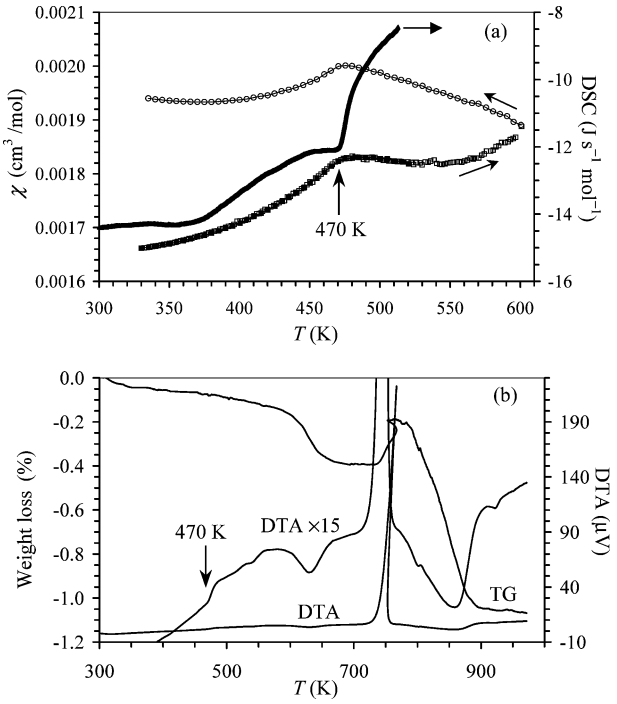

Figure 1. (a) Dependence on temperature of the magnetic susceptibility (left-hand scale) and DSC curve measured on heating (right-hand scale). The black squares are magnetic susceptibilities from 520 to 330 K, the empty squares from 330 to 600 K, and circles from 600 to 330 K. (b) TG/DTA curves of $BiCoO_3$ in air. A magnified DTA curve (×15) is also shown.

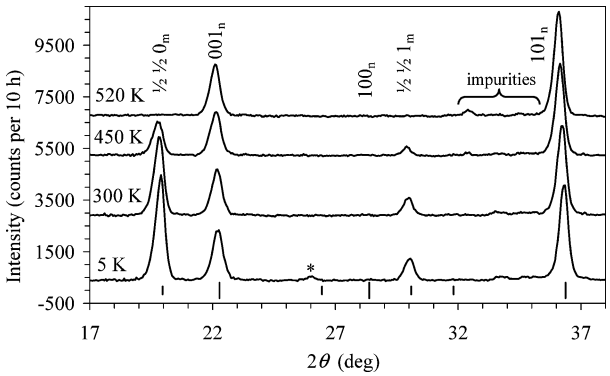

Figure 2. Neutron diffraction patterns of $BiCoO_3$ at 5, 300, 450, and 520 K in a 2θ range of 17° and 38°. Long tick marks are nuclear (n) Bragg reflections and short ones magnetic (m) Bragg reflections. Indices of reflections are given on the basis of the chemical cell with $a \approx 3.730$ Å and $c \approx 4.724$ Å. The star denotes a magnetic reflection of Co_3O_4 at 5 K (ref 24). The patterns at 300, 450, and 520 K were shifted for clarity.

indexed in a tetragonal system with $a = 3.744$ Å and $c = 4.741$ Å. Because $BiCoO_3$ is isotypic with $PbTiO_3$,[14] we used fractional coordinates of $PbTiO_3$ (space group *P*4*mm*)[23] as initial ones in the Rietveld refinements of $BiCoO_3$.

Below T_N (at 5, 300, and 450 K), strong additional reflections appeared (Figure 2). They corresponded to magnetic scattering due to antiferromagnetic order. These reflections could be indexed with doubled *a* and *b* parameters, that is, $a_m = 2a \approx 7.459$ Å and $c_m = c \approx 4.724$ Å in the tetragonal symmetry, where m denotes a magnetic cell. With this relationship between the lattice parameters of the magnetic and chemical cells, the three-dimensional long-range-ordered magnetic structure can be described in terms of a propagation vector $\mathbf{k} = (1/2, 1/2, 0)$. The magnetic reflections can be indexed on the basis of the chemical cell as $(h/2, k/2, l)$ with $h = 2n + 1$ and $k = 2n + 1$. The fact that *h* and *k* are odd implies that first nearest neighbor Co atoms within a layer have antiparallel spins. Note that, in uniaxial systems (*P*4*mm* in this case), powder diffraction cannot lead to the unambiguous determination of the magnetic moment direction in the *ab* plane; only the angle (φ) between the spin direction and the unique *c* axis can be determined.

First, we calculated the intensities of the magnetic reflections for different models of collinear antiferromagnetic arrangement of magnetic moments, assuming space group *P*1, that is, four independent Co atoms in the magnetic cell. The best agreement between the observed and calculated intensities was obtained for a model with magnetic moments parallel to the *c* axis, that is, with $\varphi = 0$. The experimental ratio between the integrated intensities of the $(1/2, 1/2, 0)$ and $(1/2, 1/2, 1)$ magnetic reflections was 4.6−4.7 at all the temperatures. The calculated ratio has a maximum for $\varphi = 0$ and decreases with increasing φ.

Then we determined the crystal structures and magnetic moments, assuming one phase with space group *P*4*mm* and a magnetic cell having lattice parameters of $a_m \approx 7.459$ Å and $c_m \approx 4.724$ Å. Because the crystal structure is described by space group *P*4*mm* with $a \approx 3.73$ Å and $c \approx 4.724$ Å, the Bi atom was fixed at $(3/4, 3/4, 0)$, structure parameters (*z* and *U*) for multiplied equivalent atoms (Co and O) were constrained to be the same, and the *x* and *y* coordinates were not refined but fixed. The following linear constraints were imposed on magnetic moments, μ, of the Co sites: $\mu(\text{Co1}) = \mu(\text{Co2}) = -\mu(\text{Co3})$ with Co1 (1a; 0, 0, $z \approx 0.566$), Co2 (1b; $1/2$, $1/2$, $z \approx 0.566$), and Co3 (2c; $1/2$, 0, $z \approx 0.566$).

For the impurity of Co_3O_4, we refined a scale factor, a lattice parameter *a*, and Gaussian profile parameters (*U*, *V*, and *W*), fixing its structure parameters.[24] The mass percentage of Co_3O_4 in the $BiCoO_3$ sample was calculated at about 6.6% from refined scale factors. For the impurity of $Bi_2O_2CO_3$, we refined a scale factor and lattice parameters (*a* and *c*), fixing its structure parameters.[25] The mass percentage of $Bi_2O_2CO_3$ in the $BiCoO_3$ sample was calculated at about 1.8%. The diffraction pattern taken at 520 K showed reflections of stainless steel (SUS) from a cryostat and additional unidentified reflections when compared with those measured at the other temperatures. Then, the SUS phase was taken into account during the refinement, and 2θ regions with the additional reflections were excluded from the refinement.

Because the sample contained a noticeable amount of Co_3O_4, the stoichiometry of $BiCoO_3$ may deviate from the ideal formula. To check this possibility, we refined the occupancies, *g*, of all the sites using the neutron diffraction data measured at all the temperatures. All the *g* parameters were unity within standard deviations. For example, at 300

(22) (a) Rangavittal, N.; Guru Row: T. N.; Rao, C. N. R. *Eur. J. Solid State Inorg. Chem.* **1994**, *31*, 409. (b) Mary, T. A.; MacKay, R.; Nguyen, P.; Sleight, A. W. *Eur. J. Solid State Inorg. Chem.* **1996**, *33*, 285.
(23) Nelmes, R. J.; Kuhs, W. F. *Solid State Commun.* **1985**, *54*, 721.
(24) Roth, W. L. *J. Phys. Chem. Solids* **1964**, *25*, 1.
(25) Grice, J. D. *Can. Miner.* **2002**, *40*, 693.

Table 1. Lattice Parameters and *R* Factors for $BiCoO_3$ at 5, 300, 450, and 520 K (Space Group *P4mm*)

	temperature			
	5 K	300 K	450 K	520 K
a (Å)	3.71990(7)	3.72937(7)	3.73797(8)	3.74432(7)
c (Å)	4.71965(15)	4.72382(15)	4.73306(16)	4.74062(15)
tetragonality, *c*/*a*	1.269	1.267	1.266	1.266
V (Å^3)	65.309(3)	65.700(3)	66.132(3)	66.463(3)
R_{wp} (%)	5.63	5.03	4.90	3.55
R_p (%)	4.11	3.69	3.60	2.65
R_B (%)[a]	2.01	1.92	1.62	2.33
R_F (%)[a]	1.08	0.95	0.97	1.21
R_B (%)[b]	9.51	8.81	13.53	
R_F (%)[b]	2.52	2.19	3.78	
S	1.58	1.38	1.33	1.69

[a] For nuclear Bragg reflections. [b] For magnetic Bragg reflections.

K, the refinement of the *g* parameters for oxygen atoms together with other variable parameters (including *U*(O1) and *U*(O2)) with fixed occupancies *g*(Bi) = 1 and *g*(Co) = 1 gave *g*(O1) = 0.996(13) and *g*(O2) = 1.004(8). The refinement of the *g* parameters for Bi and Co atoms together with other variable parameters (including *U*(Bi) and *U*(Co)) with fixed occupancies *g*(O1) = 1 and *g*(O2) = 1 resulted in *g*(Bi) = 0.997(12) and *g*(Co) = 0.994(20). These facts support no noticeable deviation from the stoichiometry of $BiCoO_3$. The *g* values were therefore fixed at unity for all the sites in the subsequent Rietveld refinements. The presence of the impurities enriched with Co can be explained in terms of the following reaction processes. That is, during melting and further decomposition of $KClO_3$, the starting mixture of Bi_2O_3 and Co_3O_4 is separated at the surface of a pellet, and Co_3O_4 penetrates more deeply into the pellet. The resultant Bi-rich impurities and KCl are removed from the surfaces of the pellets whereas Co_3O_4 remains inside the pellet. The presence of only the two phases, Co_3O_4 and "$Bi_{25}CoO_{39}$", after the decomposition of the sample shows that KCl was almost completely (within the sensitivity of XRD) removed from the surfaces.

The chemical composition of the present phases was also determined by the local EDX analysis. The results indicated that a Bi/Co ratio in the perovskite phase varied between 0.99 and 1.04, confirming the cation stoichiometry of the main phase. The grains of Co_3O_4 (a Bi-free phase according to EDX) were embedded into the grains of $BiCoO_3$. $Bi_2O_2CO_3$ (a Co-free phase according to EDX) was found as separate particles (see Supporting Information).

Table 1 gives lattice parameters and *R* factors resulting from the Rietveld refinements. Final fractional coordinates and *U* parameters in space group *P4mm* with $a \approx 3.73$ Å and $c \approx 4.724$ Å and the refined magnetic moments are listed in Table 2 and selected bond lengths, *l*, calculated with ORFFE (ref 26) in Table 3. Figure 3 displays observed, calculated, and difference neutron diffraction patterns.

The magnetic R_B factors were relatively small in comparison with values sometimes reported in the literature, for example, 17% in Li_2VOSiO_4[27] and 14 and 23% for $YBaCuFeO_5$.[28]

Table 2. Final Structure Parameters and Bond-Valence Sums (BVS) for $BiCoO_3$ at 5, 300, 450, and 520 K

		temperature			
		5 K	300 K	450 K	520 K
Bi 1a (0, 0, 0)	10^2U (Å^2)	0.04(7)	0.49(7)	0.90(7)	1.01(4)
	BVS	3.21	3.14	3.11	3.07
Co	*z*	0.5664(10)	0.5669(9)	0.5663(10)	0.5681(9)
1b ($^1/_2$, $^1/_2$, *z*)	10^2U (Å^2)	0.84(13)	1.00(13)	1.30(15)	1.58(15)
	BVS	2.68	2.68	2.68	2.66
O1	*z*	0.2024(4)	0.2034(5)	0.2064(5)	0.2073(5)
1b ($^1/_2$, $^1/_2$, *z*)	10^2U (Å^2)	0.38(7)	1.29(7)	1.94(7)	2.25(5)
	BVS	−1.58	−1.57	−1.58	−1.55
O2	*z*	0.7311(5)	0.7300(5)	0.7311(5)	0.7309(4)
2c ($^1/_2$, 0, *z*)	10^2U (Å^2)	0.28(6)	0.64(6)	0.92(7)	1.11(4)
	BVS	−2.16	−2.13	−2.10	−2.09
μ/μ_B[a]		3.24(2)	2.93(2)	1.99(2)	

[a] Magnetic moments are parallel to the *c* axis.

Table 3. Selected Bond Legnths in Å for $BiCoO_3$ at 5, 300, 450, and 520 K

	temperature			
	5 K	300 K	450 K	520 K
Bi−O2 (×4)	2.252(1)	2.259(1)	2.261(1)	2.266(1)
Bi−O1 (×4)	2.798(1)	2.807(1)	2.818(1)	2.824(1)
Co−O1	1.718(5)	1.717(5)	1.703(5)	1.711(5)
Co−O2 (×4)	2.016(2)	2.018(2)	2.025(2)	2.025(2)
Co−O1	3.002(5)	3.007(5)	3.030(5)	3.030(5)

Discussion

The neutron diffraction data unambiguously prove that $BiCoO_3$ has antiferromagnetic long-range order below T_N = 470 K. The magnetic structure is very simple with magnetic moments parallel to the *c* axis (Figures 4 and 5). The magnetic moments form the so-called C-type antiferromagnetic structure,[29] where the magnetic moments of Co^{3+} ions align antiferromagnetically in the *ab* plane, and antiferromagnetic *ab* layers stack ferromagnetically along the *c* axis. The high Néel temperature of $BiCoO_3$ provides evidence for strong interaction between Co^{3+} ions. Note that the magnetic structure found in $BiCoO_3$ has been predicted from first-principle electronic-structure calculations.[15] The same magnetic structure was predicted in $PbVO_3$ with strong antiferromagnetic interaction in the *ab* plane, $J_{ab} \approx -337$ K, and weak ferromagnetism along the *c* axis, $J_c \approx 38$ K.[15,16] However, $PbVO_3$ seems to exhibit low-dimensional magnetism in contrast with the three-dimensional long-range order in $BiCoO_3$ because magnetic susceptibilities of $PbVO_3$ demonstrate a broad maximum at about 190 K.[30]

Since $BiCoO_3$ is isotypic with $PbTiO_3$, it will show a spontaneous polarization in the tetragonal phase as predicted from the first-principle calculations.[15] The tetragonal phase of $BiCoO_3$ was found to be stable in the whole studied temperature range of 5−520 K. In ferroelectrics, the electric dipole moment can be reoriented by an external electric field, whereas pyroelectrics include materials where this reorientation does not occur. Pyroelectrics are important industrial materials along with ferroelectrics. The observation of a

(26) Busing, W. R.; Martin, K. O.; Levy H. A. *Report ORNL-TM-306*; Oak Ridge National Laboratory: Oak Ridge, TN, 1964.
(27) Bombardi, A.; Rodriguez-Carvajal, J.; Di Matteo, S.; de Bergevin, F.; Paolasini, L.; Carretta, P.; Millet, P.; Caciuffo, R. *Phys. Rev. Lett.* **2004**, *93*, 027202.
(28) (a) Caignaert, V.; Mirebeau, I.; Bourée, F.; Nguyen, N.; Ducouret, A.; Greneche, J.-M.; Raveau, B. *J. Solid State Chem.* **1995**, *114*, 24. (b) Mombru, A. W.; Prassides, K.; Christides, C.; Erwin, R.; Pissas, M.; Mitros, C.; Niarchos, D. *J. Phys.: Condens. Matter* **1998**, *10*, 1247.
(29) Wollan, E. O.; Koehler, W. C. *Phys. Rev.* **1955**, *100*, 545.
(30) Belik, A. A.; Takayama-Muromachi, E. Unpublished results.

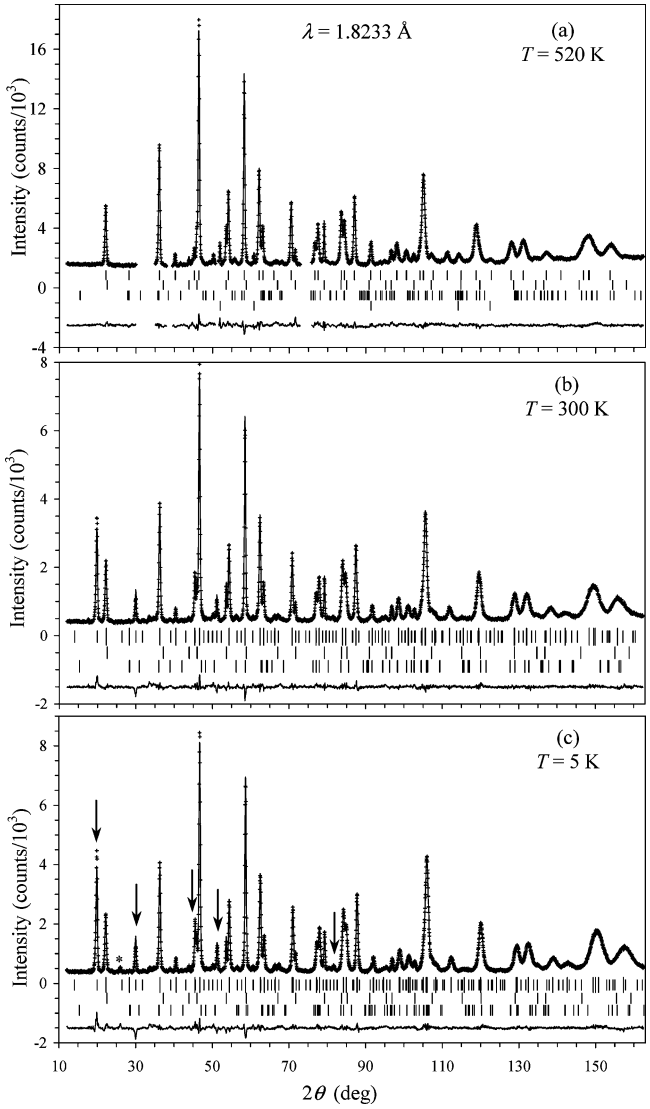

Figure 3. Observed (crosses), calculated (solid line), and difference patterns resulting from the Rietveld analysis of the neutron powder diffraction data for $BiCoO_3$ at (a) 520 K, (b) 300 K, and (c) 5 K. Bragg reflections are indicated by tick marks; the longer marks denote nuclear Bragg reflections in (b) and (c). The lower tick marks are given for the impurity phases, Co_3O_4 and $Bi_2O_2CO_3$, and SUS (at 520 K). Arrows are attached to strong magnetic reflections. The star marks the magnetic reflection of Co_3O_4 at 5 K (ref 24).

ferroelectric hysteresis loop, $P-E$, in $BiCoO_3$ seems to be problematic and probably impossible because of the marked structural distortion (and spontaneous polarization) and too low resistivity for the application of a large electric field. For example, the observation of $P-E$ hysteresis loop in $PbTiO_3$ is possible only for the samples with the resistivity above 10^{10} Ω-cm at RT. Therefore, $BiCoO_3$ should be regarded as a pyroelectric material rather than a ferroelectric one. Below 470 K, $BiCoO_3$ also has antiferromagnetically ordered magnetic moments.

The refinement of the magnetic structure for $BiCoO_3$ revealed high-spin configuration of Co^{3+} ions ($S = 2$). The reduction in the observed magnetic moment even at 5 K ($3.24(2)\mu_B$) in comparison with the expected value of $4\mu_B$ may be ascribed to the covalency of Co−O bonds. Indeed, the Co−O1 bond being much shorter than the Co−O2 one (Table 3) suggests strong covalency and partial charge

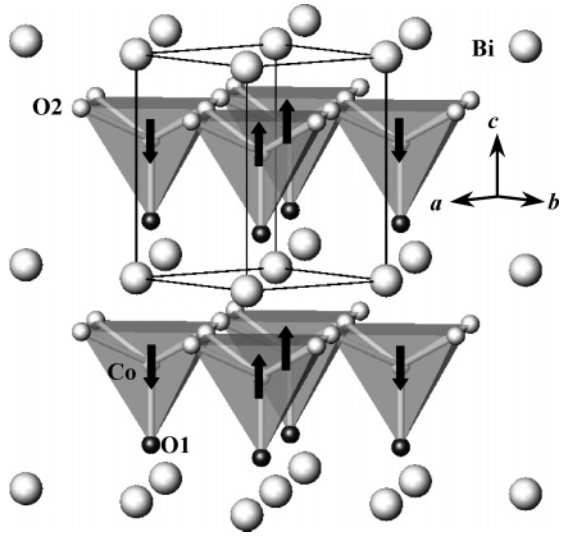

Figure 4. Crystal structure of $BiCoO_3$ with solid lines displaying the chemical cell. Arrows show the direction of the magnetic moments below $T_N = 470$ K.

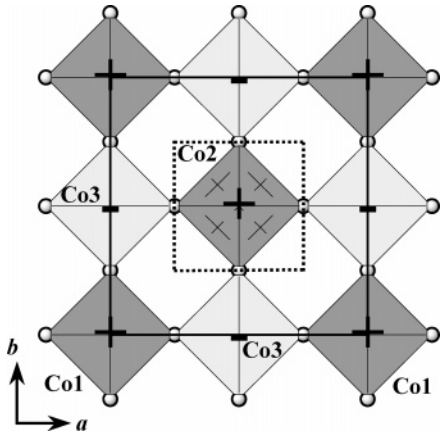

Figure 5. Crystal structure of $BiCoO_3$ viewed along the c axis; only CoO_5 polyhedra are given. The solid lines present the magnetic cell and the broken lines the chemical cell. The plus symbols denote the up alignment of the magnetic moments parallel to the c axis and the minus symbols the down alignment of the magnetic moments. The Co1, Co2, and Co3 sites were used to refine the magnetic structure in space group $P4mm$ with the lattice parameters of $a_m \approx 7.459$ Å and $c_m \approx 4.724$ Å.

transfer between O^{2-} and Co^{3+} ions. To obtain information on formal oxidation states of Bi, Co, and O, we calculated their bond valence sums, BVS,[31] in $BiCoO_3$ (Table 2). The resulting BVS values at 300 K were 3.14 for Bi and −2.13 for O2, giving the oxidation states of +3 and −2, respectively. However, the BVS values were 2.68 for Co and −1.57 for O1, which is consistent with the covalency effect. Because the magnitude of the magnetic moment of 2.93(2)μ_B at 300 K is only slightly smaller than that at 5 K, the reduction in the magnetic moment cannot be explained in terms of unsaturated behavior. The calculated magnetic moment for the C-type antiferromagnetic structure was also reduced to $2.41\mu_B$.[15]

In the case of $BiNiO_3$ with a triclinically distorted $GdFeO_3$-type structure, Ni has an oxidation state of +2; that is, its chemical formula is expressed as $Bi_{0.5}^{3+}Bi_{0.5}^{5+}Ni^{2+}O_3$.[32] Two

(31) Brese, R. E.; O'Keeffe, M. *Acta Crystallogr., Sect. B* **1991**, *47*, 192.
(32) Ishiwata, S.; Azuma, M.; Takano, M.; Nishibori, E.; Takata, M.; Sakata, M.; Kato, K. *J. Mater. Chem.* **2002**, *12*, 3733.

different Bi sites corresponding to Bi^{3+} and Bi^{5+} are included in the structure of $BiNiO_3$, which was also confirmed by BVS calculations. On the other hand, $BiCoO_3$ contains one Bi site with the oxidation state +3, as described above.

$BiCoO_3$ was found to be an insulator from the electrical-resistivity measurements (with a resistivity of about 10^5 Ω-cm at 400 K). The first-principle calculations also showed that only the G- and C-type antiferromagnetic structures are insulating with an energy gap of 0.6 eV.[15] Therefore, our experimental data confirmed the conclusion of the first-principle calculations. The resistivity of 10^{-2} Ω-cm at RT reported by Niitaka et al.[14] can be explained by a different method of preparation; namely, $KClO_4$ added as an oxygen generator was mixed together with Bi_2O_3 and Co_3O_4. Reactions of KCl with Bi_2O_3 or Co_3O_4 could result in impurities with low resistivity. In this work, we added $KClO_3$ at the bottom and top of each capsule and carefully removed the surface of the pellets.

The tetragonality of $BiCoO_3$ slightly decreased with increasing temperature (Table 1), which is similar to that of $PbTiO_3$.[33] However, the behavior of isostructural $PbVO_3$ was found to be different; the tetragonality slightly increased with increasing temperature in $PbVO_3$.[13]

Because of the presence of the heavy Bi atoms together with the light O atoms in $BiCoO_3$, the structure refinement from the neutron diffraction data is preferable to that from XRD data. In particular, neutron diffraction can give more accurate occupancies of the O sites in compounds containing heavy metals. From our structural refinements and EDX analysis, we can conclude that $BiCoO_3$ is a stoichiometric compound between 5 and 520 K without noticeable cation or oxygen deficiency.

Acknowledgment. ICYS is supported by Special Coordination Funds for Promoting Science and Technology from MEXT, Japan. We thank Dr. H. Gao of NIMS for her assistance with the SEM-EDX analysis.

Supporting Information Available: Experimental, calculated, and difference neutron powder diffraction patterns of $BiCoO_3$ at 450 K (Figure S1); the temperature dependence of resistivity (Figure S2); SEM images and the results of the EDX analysis of $BiCoO_3$ (Figure S3) (PDF). This material is available free of charge via the Internet at http://pubs.acs.org.

CM052334Z

(33) (a) Kobayashi, J.; Uesu, Y.; Sakemi, Y. *Phys. Rev. B* **1983**, *28*, 3866. (b) Mabud S. A.; Glazer, A. M. *J. Appl. Crystallogr.* **1979**, *12*, 49.